New Angles on Energy Correlators

Alipour-Fard, Samuel; Budhraja, Ankita; Thaler, Jesse; Waalewijn, Wouter J.

DOI
10.1103/l6nj-2gsh

Publication date
2025

Document Version
Final published version

Published in
Physical Review Letters

New Angles on Energy Correlators

Samuel Alipour-fard,[1,*] Ankita Budhraja,[2,†] Jesse Thaler,[1,‡] and Wouter J. Waalewijn[2,3,§]
[1]*Center for Theoretical Physics, Massachusetts Institute of Technology, Cambridge, Massachusetts 02139, USA*
[2]*Nikhef, Theory Group, Science Park 105, 1098 XG, Amsterdam, The Netherlands*
[3]*Institute for Theoretical Physics Amsterdam and Delta Institute for Theoretical Physics, University of Amsterdam, Science Park 904, 1098 XH Amsterdam, The Netherlands*

(Received 4 December 2024; revised 15 April 2025; accepted 6 May 2025; published 10 June 2025)

Energy correlators have recently come to the forefront of jet substructure studies at colliders due to their remarkable properties: they naturally separate physics at different scales, are robust to contamination from soft radiation, and offer a direct connection with quantum field theory. The current parametrization used for energy correlators, however, is based on redundant pairwise angles with complex phase space restrictions. In this Letter, we introduce a new parametrization of energy correlators that features a simpler phase space structure and preserves information about the orientation of jet constituents. Further, our parametrization drastically reduces the computational cost to compute energy correlators on experimental data; whereas the time to compute a traditional projected N-point energy correlator scales as $M^N/N!$ on a jet with M particles, our new parametrization achieves a scaling of $M^2 \ln M$, remarkably independently of N. Even for $N = 3$, this improved scaling is particularly important for studies of heavy ion collisions, and higher values of N will enable new qualitative understanding of gauge theories. Theoretical calculations for our new energy correlators differ from those of traditional parametrizations only at next-to-next-to-leading logarithmic accuracy and beyond, and we expect that our simpler phase space structure will simplify those calculations. We also discuss how to extend our parametrization to resolved N-point energy correlators that encode angular distances between greater numbers of particles, yielding intuitive visualizations of jet substructure that are qualitatively different for different jet samples. We propose two possible generalizations for probing multiprong jets and testing jet scaling behavior.

DOI: 10.1103/l6nj-2gsh

Introduction—The flow of energy within hadronic jets is an indispensable probe of quantum chromodynamics (QCD) [1–6]. Energy correlator observables [7–11] are particularly powerful tools for understanding energy flow both theoretically and experimentally [12–14]. Since energy correlators can be described directly in terms of field-theoretic energy flow operators [15–22], one can use sophisticated theoretical techniques, including the powerful technology of conformal field theories [19,23], to extract rich information about jet substructure, especially in the collinear limit [24–37].

Recent work has highlighted the role of N-point energy correlators (ENCs) in precisely understanding the fundamental structure of particle interactions. ENCs probe angular correlations between N final-state particles, which offers a simple and intuitive way to separate physics at different scales and mitigate contamination from soft radiation. Applications focused on the Large Hadron Collider (LHC) include the top quark mass [38–40], hadronization transition [41,42], dead-cone effect [43], medium modifications in heavy-ion collisions [44–51], and predictions for the energy flow of charged particles [52–55]. Energy correlators have also been used in studies of gluon saturation and nuclear tomography [56–60]. Further, energy correlators have produced the most precise jet substructure measurement of the strong coupling constant to date [13].

In this Letter, we introduce a new parametrization for energy correlators with a number of improved properties. First, our parametrization of the projected N-point energy correlator (PENC) depends on the largest distance R_1 to a "special" particle s in a set of N particles, suitably averaged over all choices for s; this yields simpler phase space restrictions than the traditional parametrization for the PENC in terms of the largest pairwise angle [25]. Second, when considering more differential information, our parametrization of resolved ENCs (RENC) employs

*Contact author: samuelaf@mit.edu
†Contact author: abudhraj@nikhef.nl
‡Contact author: jthaler@mit.edu
§Contact author: w.j.waalewijn@uva.nl

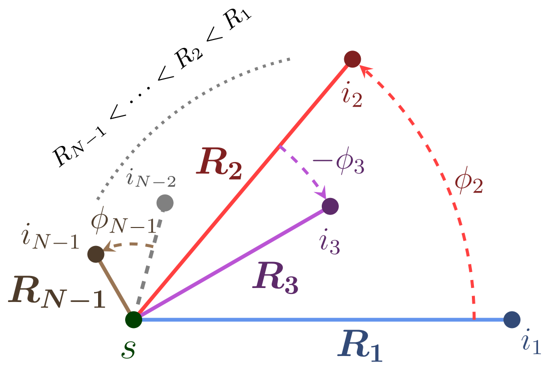

FIG. 1. An illustrative diagram of the new parametrization of ENCs we introduce in Eqs. (2) and (5). Instead of computing the ENC using all $\binom{N}{2}$ pairwise distances, we parametrize the ENC with $2N-3$ oriented polar coordinates centered on a special particle s, and then perform a momentum-weighted sum over all choices for s.

nonredundant polar coordinates centered around the special particle, as in Fig. 1, yielding intuitive visualizations of jet substructure. This differs from the traditional approach, which uses overcomplete information from the set of all pairwise distances and neglects information about the relative orientation of particles. Third, our parametrization offers dramatic improvements in computational performance, which is essential for their use in experimental analyses. Finally, we anticipate that these conceptual and computational improvements will yield simpler theoretical calculations. The implementation of the PENCs we introduce in this work can be found on GitHub as an update to FASTEEC [61], and of our PENCs and RENCs at `ResolvedEnergyCorrelators` [62].

Review of energy correlators—In proton-proton collisions—the focus of this Letter—PENCs are usually defined via [25]

$$\frac{1}{\sigma}\frac{\mathrm{d}\sigma_N}{\mathrm{d}R_L} = \left\langle \sum_{i_1\ldots i_N} z_{i_1} z_{i_2} \ldots z_{i_N} \delta(R_L - \max_{k,\ell}\{R_{i_k,i_\ell}\}) \right\rangle. \quad (1)$$

Here, $z_i = p_{T,i}/\sum_j p_{T,j}$ is the transverse momentum fraction carried by particle i in the jet, $R_{i_k,i_\ell} = \sqrt{(y_{i_k,i_\ell})^2 + (\phi_{i_k,i_\ell})^2}$ is the angular separation between particles i_k and i_ℓ in the rapidity-azimuth plane, and the angular brackets indicate an expectation value over a sample of many hadronic jets. The sum over $\{i_k\}_{k=1}^N$ indicates the sum over all sets of N particles of a jet, and the variable R_L characterizes the maximum pairwise angular separation between the i_k.

However, the expression of Eq. (1) is computationally expensive due to the intricate phase space constraint $R_L = \max_{k,\ell}\{R_{i_k,i_\ell}\}$. For example, the time required to compute the (integer) PENC scales as $M^N/N!$ for a jet with M particles; when analytically continued to noninteger values of N, the PENC suffers a computational scaling of 2^{2M} [63]. This computational cost impedes several exciting PENC applications. For example, PENCs have an approximate scaling behavior related to the Nth Mellin moment of the DGLAP splitting functions [25]; the analytic continuation of the PENC to noninteger N therefore provides access both to the full splitting functions of QCD and, in the limit $N \to 0$, a unique opportunity to study small-x physics and BFKL dynamics with jets [25,36,64]. At very large values of N, PENCs also encode additional fundamental features of QCD [25,65], such as level crossings with twist-4 operators. Furthermore, in the high-multiplicity environment of heavy ion collisions, even computing PENCs for $N = 3$ has been computationally challenging, limiting their potential in studying medium effects [51]. Improved computational efficiency is therefore necessary to leverage the full potential of PENCs in the study of realistic data samples.

Higher-point ENCs also yield more detailed shape information about the structure of radiation inside jets. For example, recent work has leveraged the E3C to propose a new method for extracting the top quark mass from experimental data [38–40]. Notably, for $N > 3$ the parametrization of ENCs in terms of the R_{i_k,i_ℓ} is overcomplete: the R_{i_k,i_ℓ} describe $\binom{N}{2}$ distances, while only $2N-3$ are independent.

New angles: The projected case—In this Letter, we introduce a new parametrization of PENCs with a simpler phase space structure:

$$\frac{1}{\sigma}\frac{\mathrm{d}\sigma_N}{\mathrm{d}R_1} = \left\langle \sum_{s=1}^{M} z_s \sum_{i_1\ldots i_{N-1}} z_{i_1}\ldots z_{i_{N-1}} \delta(R_1 - \max_j\{R_{s,i_j}\}) \right\rangle,$$
$$\equiv \mathrm{PENC}(R_1). \quad (2)$$

The sums on s and $\{i_j\}_{j=1}^{N-1}$ again run over all M particles within a jet. The crucial simplification is that our PENC is based on a new variable, R_1, that indicates the maximum distance $\max\{R_{s,i_j}\}$ between the *single* particle s and any of the remaining $N-1$ particles $\{i_j\}_{j=1}^{N-1}$.

Like the old variable R_L of Eq. (1), R_1 still roughly characterizes the maximum angular scale between a set of N particles, since $R_L/2 \le R_1 \le R_L$ by the triangle inequality. Indeed, the PENCs displayed in Fig. 2 show that the difference between our parametrization and that of Eq. (1) is small, and that both parametrizations have similar scaling behavior in the perturbative region (though there are some differences in the perturbative to nonperturbative transition). Figures 2–4 all feature energy correlators evaluated on the CMS 2011A Jet Primary Dataset [66,67], also available in MIT Open Data format [68,69], on anti-k$_t$ jets with transverse momenta $p_T^{\mathrm{jet}} \in [500, 550]$ GeV and pseudorapidity $|\eta^{\mathrm{jet}}| < 1.9$ [70].

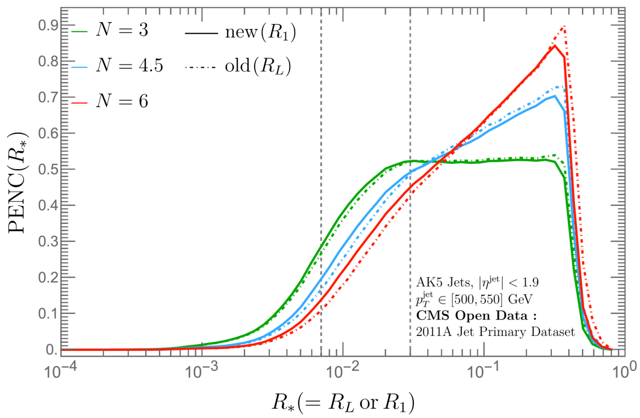

FIG. 2. PENC distributions for $N = \{3, 4.5, 6\}$, calculated using our new parametrization (solid) and the traditional parametrization (dashed). R_* denotes the largest distance to the special particle for our new parametrization (R_1), and the largest separation between the N particles for the traditional one (R_L). The differences are small in the perturbative region $R_* \gg \Lambda_{QCD}/p_T$, but become noticeable in the transition between perturbative and nonperturbative regimes (indicated by the vertical dashed lines).

Improved computation time—The computational efficiency of our parametrization is more evident in the (normalized) cumulative distribution:

$$\Sigma_N(R_1) = \frac{1}{\sigma}\int_0^{R_1} dR_1' \frac{d\sigma_N}{dR_1'} = \left\langle \sum_s z_s [z_{\rm disk}(s, R_1)]^{N-1} \right\rangle, \quad (3)$$

where $z_{\rm disk}(s, R_1)$ denotes the total transverse momentum fraction of all particles within a radius R_1 of the special particle s. Notably, the simple form of Eq. (3) holds even for noninteger N. A practical way to evaluate Eq. (3) [and Eq. (2) after differentiation] is, for each s, to first sort all particles by their distance with respect to s, and then to compute $\Sigma_N(R_1)$ by beginning with $R_1 = 0$ and then increasing it. Sorting particles by their distance to s takes $M \ln M$ time, and the remaining sum over s scales with M, resulting in an overall computation time scaling as $M^2 \ln M$. This computational speedup is especially interesting for heavy-ion collisions where M is typically very large. We illustrate the dramatic improvement in the computation time for higher-point energy correlators in Supplemental Material.

Theoretical perspectives—The factorization formula for the traditional PENCs [25] also applies to our new PENCs, with one small difference: because the variables R_1 and R_L differ for three or more emissions, the jet function for our PENCs differs from the old one at $\mathcal{O}(\alpha_s^2)$, or at next-to-next-to-leading logarithmic accuracy (NNLL). In Supplemental Material, we discuss how the NLL equivalence of jet functions implies that $\Sigma_N(R_L) = \Sigma_N(R_1 = R_L[1 + \mathcal{O}(\alpha_s)])$ [71]. Furthermore, at NNLL and beyond, we expect that the simple dependence of Eq. (3) on N will substantially simplify the calculation of the jet function for R_1. By contrast, the jet function using the old parametrization requires dedicated calculations for each individual value of N [24,31].

Finally, we note that Eq. (3) is the Nth Mellin moment in z of

$$\frac{1}{\sigma}\frac{d\sigma}{dz}(R_1) = \left\langle \sum_s z_s \delta[z - z_{\rm disk}(s, R_1)] \right\rangle, \quad (4)$$

which is also the differential jet rate in a jets-without-jets approach if R_1 is treated as a jet radius [73,74]. A similar moment relation between the jet rate and the original ENC was noted in Ref. [75].

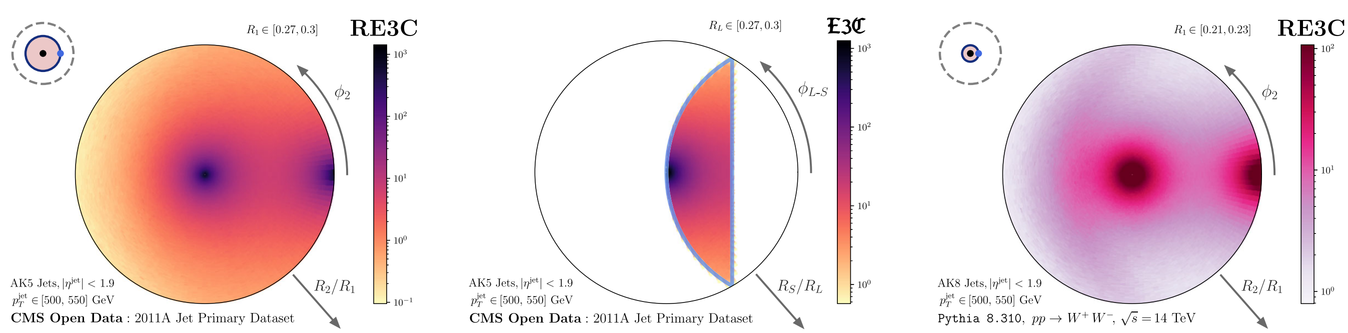

(a) (b) (c)

FIG. 3. Polar heat maps visualizing (a) our new RE3C applied to CMS Open Data, (b) the traditional E3C applied to CMS Open Data, and (c) our new parametrization applied to W-boson-initiated jets from PYTHIA 8.310. In (a) and (c), the radial variables correspond to R_2/R_1, the polar angle corresponds to ϕ_2, and we show the RE3C in the bin $R_1 \in [0.27, 0.3]$. In (b) the radius corresponds to R_S/R_L, the polar angle corresponds to the angle between associated lines of length R_S and R_L, and we show the E3C in the bin $R_L \in [0.27, 0.3]$. In all three plots, we see collinear enhancements for the RE3C near the origin, when two particles become very close in angle. In (a) and (c), we also see collinear enhancements as $R_2/R_1 \to 1$ and $\phi_2 \to 0$, and (c) exhibits additional noncollinear enhancements correlated with the W-boson mass.

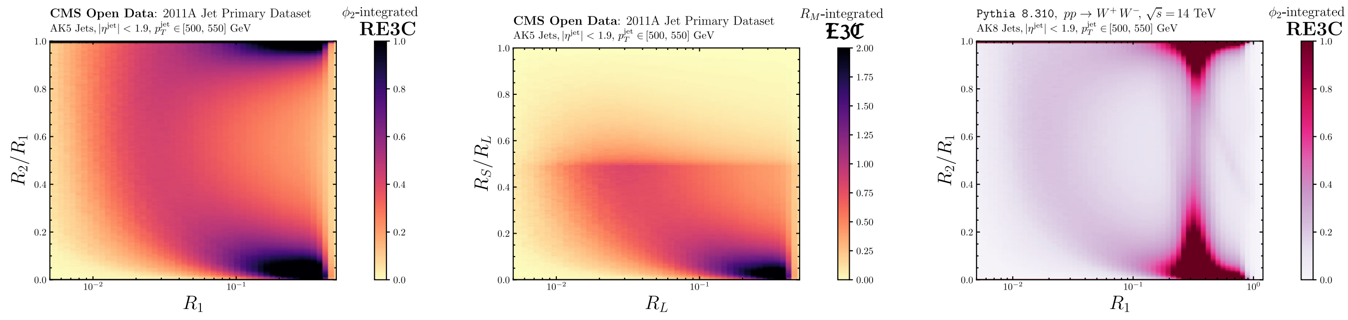

(a) (b) (c)

FIG. 4. Normalized distributions (a) our new RE3C applied to CMS Open Data when integrated over the azimuthal angle ϕ_2, (b) the traditional E3C applied to CMS Open Data integrated over the intermediate angle R_M (analogous to integrating over ϕ_s), and (c) our new, ϕ_2-integrated RE3C applied to W-boson-initiated jets.

New angles: The general case—By including (or *resolving*) more detailed angular information about the positions and relative orientations of particles within the jet, we may generalize our new parametrization for the PENC to introduce the RENC:

$$\begin{aligned}
&\mathrm{RENC}(R_1, R_2, \phi_2, R_3, \phi_3, \ldots) \\
&\equiv \frac{1}{\sigma} \frac{\mathrm{d}\sigma_N}{\mathrm{d}R_1 \mathrm{d}R_2 \mathrm{d}\phi_2 \mathrm{d}R_3 \mathrm{d}\phi_3 \ldots} \\
&= \Big\langle \sum_s z_s \sum_{i_1 \geq \ldots \geq i_{N-1}} z_{i_1} \ldots z_{i_{N-1}} \binom{N}{n_1 n_2 \ldots} \delta(R_1 - R_{s,i_1}) \\
&\quad \times \rho_{i_2}(R_2, \phi_2) \rho_{i_3}(R_3, \phi_3) \ldots \Big\rangle, \qquad (5)
\end{aligned}$$

where for each s, the i_j are indexed such that $R_{s,i_1} \geq R_{s,i_2} \geq \ldots$, and the summand involves the per-particle densities:

$$\rho_{i_j}(R_j, \phi_j) = \delta(R_j - R_{s,i_j}) \delta(\phi_j - \phi_{i_{j-1},i_j}). \qquad (6)$$

The "…" correspond to additional R_j and ϕ_j, and n_k denotes how often particle k of the jet appears among the i_j (such that terms with $n_k > 1$ encode self-correlations of particle k), with $\sum_{k=1}^{M} n_k = N$.

Our parametrization is visualized in Fig. 1, and utilizes polar coordinates around s, ordered in radius $R_1 > R_2 > \ldots$ and with an *oriented* azimuthal angle ϕ_j taken relative to the $(j-1)$th resolved emission. The R_j and ϕ_j use $2N-3$ variables to completely characterize the positions of all particles in the jet, relative to the axis defined by particles s and i_1. The multinomial coefficient in Eq. (5) arises due to the ordering of the R_j, and accounts for the possibility that two or more of the i_j may be equal. Integrating inclusively over $\{R_j, \phi_j\}_{j=2}^{N}$ [which sets the third line of Eq. (5) to unity] reduces the RENC to the PENC from Eq. (2).

The RENCs we introduce also preserve information about relative orientations, whereas even in the simple example of $N = 3$, the traditional E3C parametrization in terms of the largest (R_L), medium (R_M), and shortest (R_S) distances does not. We visualize the additional orientation information preserved by our RE3Cs in Figs. 3(a) and 3(b), where we compare polar heat maps of our parametrization of the RE3C to the traditional paramterization of the E3C. The additional angular information carried by our new RE3C also leads to striking visual differences when comparing jets initiated by different processes. For example, the unique characteristics of the RE3C evaluated on W-boson initiated jets generated with PYTHIA 8.310 [76,77], shown in Fig. 3(c), clearly distinguish it from the RE3C of QCD-initiated jets. This qualitative difference is not visible in the traditional parametrization, as shown in Supplemental Material [71] together with similar visualizations for additional processes.

The squeezed limit of our new RE3C, $R_2 \ll R_1$, is quite similar to the squeezed limit of the traditional E3C, $R_S \ll R_L$; in this limit, $R_2 \sim R_S$ and $R_1 \sim R_L$. Our new RE3C and the traditional E3C evaluated on CMS Open Data are compared in Figs. 4(a) and 4(b), which demonstrate that they indeed take similar forms when $R_S/R_L, R_2/R_1 < \frac{1}{2}$. When $R_S/R_L > \frac{1}{2}$, however, the traditional E3C is suppressed due to the hierarchy $R_S < R_M < R_L$. In Fig. 4(c), we visualize our new RE3C on PYTHIA-generated W jets, which exhibits a nonperturbative ridge similar to the one seen in CMS Open Data as well as additional features at $R_1 = 0.3$ correlated with the W mass, $R_1 \sim 2m_W/p_T$. In Supplemental Material [71], we explain the ridgelike features in these plots from the perspective of nonperturbative physics.

Finally, we note that each additional resolved particle [i.e., each (R_j, ϕ_j) pair] introduces a factor of M to the scaling of the RENC computation time. In contrast, the computation time for, e.g., the traditional 4-point correlator scales as M^4 independent of how many angles were resolved.

Generalizations—For completeness, we mention two additional generalizations of our new parametrization for energy correlators—RENCs with two special particles and

RENCs with two projected angles—for which we defer more detailed explorations to future work. For the energy correlator with two special particles,

$$\frac{1}{\sigma}\frac{d\sigma_{N,N'}}{dR dR_1 dR'_1} = \Big\langle \sum_s z_s \sum_{s'} z_{s'} \delta(R - R_{ss'}) \times \sum_{i_1\ldots i_{N-1}} z_{i_1}\ldots z_{i_{N-1}} \delta(R_1 - \max\{R_{s,i_k}\}) \times \sum_{j_1\ldots j_{N'-1}} z_{j_1}\ldots z_{j_{N'-1}} \delta(R'_1 - \max\{R_{s',j_k}\}) \Big\rangle, \tag{7}$$

the two special particles s and s' are separated by a distance R, and R_1 and R'_1 denote the maximum distance of other particles to s and s', respectively. This parametrization may capture interesting features of the radiation patterns of intrinsically 2-prong jets, e.g., from the hadronic decays of W or Higgs bosons, with a straightforward extension to three or more special particles for higher-prong jets.

We also define a *double*-projected energy-correlator,

$$\frac{1}{\sigma}\frac{d\sigma_{(a,b)}}{dR_1 dR_2} = \Big\langle \sum_s z_s \sum_{i_1\ldots i_a} z_{i_1}\ldots z_{i_a} \delta(R_1 - \max\{R_{s,i_k}\}) \times \sum_{j_1\ldots j_b} z_{j_1}\ldots z_{j_b} \delta(R_2 - \max\{R_{s,j_k}\}) \Big\rangle, \tag{8}$$

where one would typically take $R_1 > R_2$. The associated cumulative distribution, analogous to Eq. (3), is

$$\Sigma_{(a,b)}(R_1, R_2) = \frac{1}{\sigma}\int_0^{R_1} dR'_1 \int_0^{R_2} dR'_2 \frac{d\sigma_{a,b}}{dR'_1 dR'_2} = \Big\langle \sum_s z_s [z_{\rm disk}(s, R_1)]^a [z_{\rm disk}(s, R_2)]^b \Big\rangle, \tag{9}$$

highlighting that there is no additional complication when a, b are noninteger. Because the effective scaling of this observable is set by $N = 1 + a + b$ and because the $N = 1$ moment of the DGLAP splitting functions vanish, we expect very mild dependence on R_1 at fixed R_2/R_1 when $b = -a$. This behavior therefore offers an interesting test of parton shower generators.

Discussion and outlook—Motivated by existing results and the tremendous potential of energy correlators for the characterization of jet substructure, this Letter introduces a new parametrization for higher-point correlators with several distinct advantages for both theoretical and data-driven analyses. Our new parametrization exhibits dramatically improved computational efficiency when evaluated on experimental data (without approximations), preserves information about the parity and relative orientation between particles within jets, and has intuitive features that benefit data visualization. We also expect that the simplified phase space will streamline theoretical calculations, the inclusion of hadronization effects, and pileup subtraction. Additionally, our parametrization does not involve any redundancy of phase space variables, unlike traditional parametrizations. We anticipate that the reparametrization of energy correlators we introduce in this Letter will benefit current studies of energy flow within hadronic jets and open new avenues for the use of energy correlators in the study of particle collisions.

Acknowledgments—We thank Kyle Lee, Ian Moult, and Aditya Pathak for inspiring discussions. J. T. thanks Arjun Kudinoor, Yen-Jie Lee, and Krishna Rajagopal for conversations about computational and visualization challenges with the traditional ENC parametrization. A. B. is supported by the project “Microscopy of the Quark Gluon Plasma Using High-Energy Probes” (Project No. VI. C.182.054), which is partly financed by the Dutch Research Council (NWO). S. A. F. and J. T. are supported by the U.S. DOE Office of High Energy Physics under Grant No. DE-SC0012567. J. T. is additionally supported by the Simons Foundation through Investigator Grant No. 929241. W. W. would like to thank the MIT CTP, where this work was initiated, for hospitality.

[1] James D. Bjorken and Stanley J. Brodsky, Statistical model for electron-positron annihilation into hadrons, Phys. Rev. D **1**, 1416 (1970).

[2] Howard Georgi and Marie Machacek, Simple quantum-chromodynamics prediction of jet structure in e^+e^- annihilation, Phys. Rev. Lett. **39**, 1237 (1977).

[3] Edward Farhi, Quantum chromodynamics test for jets, Phys. Rev. Lett. **39**, 1587 (1977).

[4] G. Parisi, Superinclusive cross sections, Phys. Lett. **74B**, 65 (1978).

[5] John F. Donoghue, F. E. Low, and So-Young Pi, Tensor analysis of hadronic jets in quantum chromodynamics, Phys. Rev. D **20**, 2759 (1979).

[6] P. E. L. Rakow and B. R. Webber, Transverse momentum moments of hadron distributions in QCD jets, Nucl. Phys. **B191**, 63 (1981).

[7] George F. Sterman, Jet structure in e^+e^- annihilation with massless hadrons, Report No. ILL-TH-75-32, 1975, https://inspirehep.net/literature/100933.

[8] C. Louis Basham, Lowell S. Brown, S. D. Ellis, and S. T. Love, Electron-positron annihilation energy pattern in quantum chromodynamics: Asymptotically free perturbation theory, Phys. Rev. D **17**, 2298 (1978).

[9] C.Louis Basham, Lowell S. Brown, Stephen D. Ellis, and Sherwin T. Love, Energy correlations in electron-positron annihilation: Testing QCD, Phys. Rev. Lett. **41**, 1585 (1978).

[10] C. L. Basham, L. S. Brown, S. D. Ellis, and S. T. Love, Energy correlations in electron-positron annihilation in quantum chromodynamics: Asymptotically free perturbation theory, Phys. Rev. D **19**, 2018 (1979).

[11] C. Louis Basham, Lowell S. Brown, Stephen D. Ellis, and Sherwin T. Love, Energy correlations in perturbative quantum chromodynamics: A conjecture for all orders, Phys. Lett. **85B**, 297 (1979).
[12] Marianna Mazzilli (ALICE Collaboration), Measurements of HF-tagged jet substructure and energy-energy correlators with ALICE, Proc. Sci. EPS-HEP2023 (**2024**) 262.
[13] Aram Hayrapetyan *et al.* (CMS Collaboration), Measurement of energy correlators inside jets and determination of the strong coupling $\alpha_S(m_Z)$, Phys. Rev. Lett. **133**, 071903 (2024).
[14] Andrew Tamis (STAR Collaboration), Measurement of two-point energy correlators within1 jets in ***p p*** collisions at $\sqrt{s} = 200$ GeV at STAR, Proc. Sci. HardProbes2023 (**2024**) 175 [arXiv:2309.05761].
[15] N. A. Sveshnikov and F. V. Tkachov, Jets and quantum field theory, Phys. Lett. B **382**, 403 (1996).
[16] Fyodor V. Tkachov, Measuring multi-jet structure of hadronic energy flow or what is a jet?, Int. J. Mod. Phys. A **12**, 5411 (1997).
[17] Gregory P. Korchemsky and George F. Sterman, Power corrections to event shapes and factorization, Nucl. Phys. **B555**, 335 (1999).
[18] Christopher Lee and George F. Sterman, Momentum flow correlations from event shapes: Factorized soft gluons and soft-collinear effective theory, Phys. Rev. D **75**, 014022 (2007).
[19] Diego M. Hofman and Juan Maldacena, Conformal collider physics: Energy and charge correlations, J. High Energy Phys. 05 (2008) 012.
[20] A. V. Belitsky, S. Hohenegger, G. P. Korchemsky, E. Sokatchev, and A. Zhiboedov, From correlation functions to event shapes, Nucl. Phys. **B884**, 305 (2014).
[21] A. V. Belitsky, S. Hohenegger, G. P. Korchemsky, E. Sokatchev, and A. Zhiboedov, Event shapes in $\mathcal{N} = 4$ super-Yang-Mills theory, Nucl. Phys. **B884**, 206 (2014).
[22] Petr Kravchuk and David Simmons-Duffin, Light-ray operators in conformal field theory, J. High Energy Phys. 11 (2018) 102.
[23] Murat Kologlu, Petr Kravchuk, David Simmons-Duffin, and Alexander Zhiboedov, The light-ray OPE and conformal colliders, J. High Energy Phys. 01 (2021) 128.
[24] Lance J. Dixon, Ian Moult, and Hua Xing Zhu, Collinear limit of the energy-energy correlator, Phys. Rev. D **100**, 014009 (2019).
[25] Hao Chen, Ian Moult, XiaoYuan Zhang, and Hua Xing Zhu, Rethinking jets with energy correlators: Tracks, resummation, and analytic continuation, Phys. Rev. D **102**, 054012 (2020).
[26] Hao Chen, Ming-Xing Luo, Ian Moult, Tong-Zhi Yang, Xiaoyuan Zhang, and Hua Xing Zhu, Three point energy correlators in the collinear limit: Symmetries, dualities and analytic results, J. High Energy Phys. 08 (2020) 028.
[27] Hao Chen, Ian Moult, and Hua Xing Zhu, Quantum interference in jet substructure from spinning gluons, Phys. Rev. Lett. **126**, 112003 (2021).
[28] Hao Chen, Ian Moult, and Hua Xing Zhu, Spinning gluons from the QCD light-ray OPE, J. High Energy Phys. 08 (2022) 233.
[29] Stella T. Schindler, Iain W. Stewart, and Zhiquan Sun, Renormalons in the energy-energy correlator, J. High Energy Phys. 10 (2023) 187.
[30] Anjie Gao, Hai Tao Li, Ian Moult, and Hua Xing Zhu, The transverse energy-energy correlator at next-to-next-to-next-to-leading logarithm, J. High Energy Phys. 09 (2024) 072.
[31] Wen Chen, Jun Gao, Yibei Li, Zhen Xu, Xiaoyuan Zhang, and Hua Xing Zhu, NNLL resummation for projected three-point energy correlator, J. High Energy Phys. 05 (2024) 043.
[32] Dmitry Chicherin, Ian Moult, Emery Sokatchev, Kai Yan, and Yunyue Zhu, The collinear limit of the four-point energy correlator in $\mathcal{N} = 4$ super Yang-Mills theory, Phys. Rev. D **110**, L091901 (2024).
[33] Hao Chen, Pier Francesco Monni, Zhen Xu, and Hua Xing Zhu, Scaling violation in power corrections to energy correlators from the light-ray OPE, Phys. Rev. Lett. **133**, 231901 (2024).
[34] Cyuan-Han Chang and David Simmons-Duffin, Three-point energy correlators and the celestial block expansion, J. High Energy Phys. 02 (2023) 126.
[35] Ankita Budhraja and Wouter J. Waalewijn, FASTEEC: Fast evaluation of N-point energy correlators, Phys. Lett. B **861**, 139276 (2025).
[36] Ankita Budhraja, Hao Chen, and Wouter J. Waalewijn, ν-point energy correletors with FASTEEC: Small-x physics from LHC jets, Phys. Lett. B **861**, 139239 (2025).
[37] Kyle Lee, Francesco Turro, and Xiaojun Yao, Quantum computing for energy correlators, Phys. Rev. D **111**, 054514 (2025).
[38] Jack Holguin, Ian Moult, Aditya Pathak, and Massimiliano Procura, New paradigm for precision top physics: Weighing the top with energy correlators, Phys. Rev. D **107**, 114002 (2023).
[39] Jack Holguin, Ian Moult, Aditya Pathak, Massimiliano Procura, Robert Schöfbeck, and Dennis Schwarz, Using the W as a standard candle to reach the top: Calibrating energy correlator based top mass measurements, arXiv:2311.02157.
[40] Jack Holguin, Ian Moult, Aditya Pathak, Massimiliano Procura, Robert Schöfbeck, and Dennis Schwarz, Top quark mass extractions from energy correlators: A feasibility study, J. High Energy Phys. 04 (2025) 072.
[41] Patrick T. Komiske, Ian Moult, Jesse Thaler, and Hua Xing Zhu, Analyzing N-point energy correlators inside jets with CMS open data, Phys. Rev. Lett. **130**, 051901 (2023).
[42] Kyle Lee, Aditya Pathak, Iain Stewart, and Zhiquan Sun, Nonperturbative effects in energy correlators: From characterizing confinement transition to improving α_s extraction, Phys. Rev. Lett. **133**, 231902 (2024).
[43] Evan Craft, Kyle Lee, Bianka Meçaj, and Ian Moult, Beautiful and charming energy correlators, arXiv:2210.09311.
[44] Carlota Andres, Fabio Dominguez, Raghav Kunnawalkam Elayavalli, Jack Holguin, Cyrille Marquet, and Ian Moult, Resolving the scales of the quark-gluon plasma with energy correlators, Phys. Rev. Lett. **130**, 262301 (2023).
[45] Carlota Andres, Fabio Dominguez, Jack Holguin, Cyrille Marquet, and Ian Moult, A coherent view of the quark-gluon plasma from energy correlators, J. High Energy Phys. 09 (2023) 088.

[46] João Barata, José Guilherme Milhano, and Andrey V. Sadofyev, Picturing QCD jets in anisotropic matter: from jet shapes to energy energy correlators, Eur. Phys. J. C **84**, 174 (2024).

[47] João Barata, Paul Caucal, Alba Soto-Ontoso, and Robert Szafron, Advancing the understanding of energy-energy correlators in heavy-ion collisions, J. High Energy Phys. 11 (2024) 060.

[48] Carlota Andres, Fabio Dominguez, Jack Holguin, Cyrille Marquet, and Ian Moult, Seeing beauty in the quark-gluon plasma with energy correlators, Phys. Rev. D **110**, L031503 (2024).

[49] Balbeer Singh and Varun Vaidya, Factorization for energy-energy correlator in heavy ion collision, arXiv:2408.02753.

[50] CMS Collaboration, Energy-energy correlators from PbPb and pp collisions at 5.02 TeV, Report No. CMS-PAS-HIN-23-004, 2024, https://inspirehep.net/literature/2817909.

[51] Hannah Bossi, Arjun Srinivasan Kudinoor, Ian Moult, Daniel Pablos, Ananya Rai, and Krishna Rajagopal, Imaging the wakes of jets with energy-energy-energy correlators, J. High Energy Phys. 12 (2024) 073.

[52] Yibei Li, Ian Moult, Solange Schrijnder van Velzen, Wouter J. Waalewijn, and Hua Xing Zhu, Extending precision perturbative QCD with track functions, Phys. Rev. Lett. **128**, 182001 (2022).

[53] Hao Chen, Max Jaarsma, Yibei Li, Ian Moult, Wouter J. Waalewijn, and Hua Xing Zhu, Collinear parton dynamics beyond DGLAP, Phys. Rev. D **111**, 076021 (2025).

[54] Hao Chen, Max Jaarsma, Yibei Li, Ian Moult, Wouter J. Waalewijn, and Hua Xing Zhu, Multi-collinear splitting kernels for track function evolution, J. High Energy Phys. 07 (2023) 185.

[55] Max Jaarsma, Yibei Li, Ian Moult, Wouter J. Waalewijn, and Hua Xing Zhu, Energy correlators on tracks: Resummation and non-perturbative effects, J. High Energy Phys. 12 (2023) 087.

[56] G. Karapetyan, Nuclear configurational entropy of the energy-energy correlation in e^+e^- annihilation processes, Europhys. Lett. **125**, 58001 (2019).

[57] Xiaohui Liu and Hua Xing Zhu, Nucleon energy correlators, Phys. Rev. Lett. **130**, 091901 (2023).

[58] Hao-Yu Liu, Xiaohui Liu, Ji-Chen Pan, Feng Yuan, and Hua Xing Zhu, Nucleon energy correlators for the color glass condensate, Phys. Rev. Lett. **130**, 181901 (2023).

[59] Zhong-Bo Kang, Kyle Lee, Ding Yu Shao, and Fanyi Zhao, Collins-type energy-energy correlators and nucleon structure, in *Proceedings of the 30th International Workshop on Deep-Inelastic Scattering and Related Subjects* (2023), arXiv:2307.06935.

[60] Haotian Cao, Xiaohui Liu, and Hua Xing Zhu, Toward precision measurements of nucleon energy correlators in lepton-nucleon collisions, Phys. Rev. D **107**, 114008 (2023).

[61] Ankita Budhraja and Wouter Waalewijn, FASTEEC 0.2 (2024), https://github.com/abudhraj/FastEEC/releases/tag/0.2.

[62] Samuel Alipour-fard, `ResolvedEnergyCorrelators` (RENCs), https://github.com/samcaf/ResolvedEnergyCorrelators (2024).

[63] FASTEEC [35] achieves a substantial speed up by replacing particles with subjets whose radius is chosen dynamically, depending on the desired level of angular resolution. For non-integer N, FASTEEC furthermore uses a recursive algorithm that reduces the standard 2^{2M} scaling down to $M2^M$ [36].

[64] Duff Neill and Felix Ringer, Soft fragmentation on the celestial sphere, J. High Energy Phys. 06 (2020) 086.

[65] Lin Dai, Chul Kim, and Adam K. Leibovich, Large N-point energy correlator in the collinear limit, arXiv:2410.11614.

[66] CERN Open Data Portal, http://opendata.cern.ch.

[67] CMS Collaboration, Jet primary dataset in AOD format from RunA of 2011 (/Jet/Run2011A-12Oct2013-v1/AOD), CERN Open Data Portal (2016), 10.7483/OPENDATA.CMS.UP77.P6PQ.

[68] Patrick T. Komiske, Radha Mastandrea, Eric M. Metodiev, Preksha Naik, and Jesse Thaler, Exploring the space of jets with CMS open data, Phys. Rev. D **101**, 034009 (2020).

[69] Patrick Komiske, Radha Mastandrea, Eric Metodiev, Preksha Naik, and Jesse Thaler, CMS 2011A Open Data ||Jet Primary Dataset || pT > 375 GeV||MOD HDF5 Format (2019), http://dx.doi.org/10.5281/zenodo.3340205.

[70] Matteo Cacciari, Gavin P. Salam, and Gregory Soyez, The anti-k_t jet clustering algorithm, J. High Energy Phys. 04 (2008) 063.

[71] See Supplemental Material at http://link.aps.org/supplemental/10.1103/l6nj-2gsh, which includes Ref. [72], which we used to verify the relation in terms of quantiles.

[72] Jasmine Brewer, José Guilherme Milhano, and Jesse Thaler, Sorting out quenched jets, Phys. Rev. Lett. **122**, 222301 (2019).

[73] Daniele Bertolini, Tucker Chan, and Jesse Thaler, Jet observables without jet algorithms, J. High Energy Phys. 04 (2014) 013.

[74] Daniele Bertolini, Jesse Thaler, and Jonathan R. Walsh, The first calculation of fractional jets, J. High Energy Phys. 05 (2015) 008.

[75] Kyle Lee, Ian Moult, and Xiaoyuan Zhang, Revisiting single inclusive jet production: Timelike factorization and reciprocity, arXiv:2409.19045.

[76] Christian Bierlich *et al.*, A comprehensive guide to the physics and usage of PYTHIA 8.3, SciPost Phys. Codebases **2022**, 8 (2022).

[77] Peter Skands, Stefano Carrazza, and Juan Rojo, Tuning PYTHIA 8.1: The Monash 2013 tune, Eur. Phys. J. C **74**, 3024 (2014).